

## RESEARCH ARTICLE

# Simulation and visualization of adapting venation patterns

Monssef Alsweis<sup>1\*</sup>, Oliver Deussenn<sup>1,2</sup> and Jia Liu<sup>3</sup><sup>1</sup> Department of Computer Information Science, University of Konstanz, Konstanz, Germany<sup>2</sup> SIAT, Chinese Academy of Science, Shenzhen, China<sup>3</sup> School of Automation, Beijing Information Science Technology University, Beijing, China

## ABSTRACT

This paper suggests a procedural biologically motivated method to simulate the development of leaf contours and the generation of different levels of leaf venation systems. Leaf tissue is regarded as a viscous, incompressible fluid whose 2D expansion is determined by a spatially varying growth rate. Visually realistic development is described by a growth function relative elementary growth rate that reacts to hormone (Auxin) sources embedded in the leaf blade. The shape of the leaf is determined by a set of feature points at the leaf contour. The contour is extracted from images utilizing the curvature scale space corner detection algorithm. Auxin transport is described by an initial Auxin flow from a source to a sink that is gradually channelized into cells with large amounts of highly polarized transporters. The proposed model simulates leaf forms ranging from simple shapes to lobed leaves. The third level of venation system is generated using centroidal Voronoi tessellations and minimum spanning trees, whereas the size of each cell within the Voronoi-diagram is related to the involved quantity of Auxin. Copyright © 2016 John Wiley & Sons, Ltd.

## KEYWORDS

leaf development; Auxin; curvature scale space; botanical simulation;  $\mathbb{R}ER\mathbb{G}$ ; centroidal Voronoi tessellations; minimum spanning tree

## \*Correspondence

Monssef Alsweis, Department of Computer Information Science, University of Konstanz, Universitätsstraße 10, 78464 Konstanz, Germany.

E-mail: monssef.alsweis@uni-konstanz.de

## 1. INTRODUCTION

While the modeling of complex plants in general received lots of attention in computer graphics, the modeling of growing plant leaves has been investigated only to a limited extent. This is interesting because leaf forms and vascular patterns provide some of the most impressive examples of the complexity of biological shapes generated in nature. Furthermore, plant and leaf simulations have a long history in bridging biology, theoretical studies of morphogenesis, and botanical visualization [1].

In this paper, a mathematical model is presented to simulate the growth of leaves. The tissue of the leaf is regarded as a viscous, incompressible fluid whose two-dimensional (2D) expansion is caused by a spatially varying growth rate [2]. We propose a physically based approach to model a leaf based on the corresponding expansion rate [3]. We ignore body forces such as gravity and only assume surface forces.

We describe growth by using a growth tensor field as proposed by [4–6]. The growth tensor allows full characterization of the growth rate in length, area, and volume; it describes the rates of angular changes between elements and of vorticity. The growth tensor is a generalization of the relative elementary growth rates ( $\mathbb{R}ER\mathbb{G}$ )  $\mathbb{R}ER\mathbb{G}_x$ ,  $\mathbb{R}ER\mathbb{G}_y$ , and  $\mathbb{R}ER\mathbb{G}_z$  along the main axes of a leaf. The growth rate of a plant leaf is a scalar or a vector quantity. This vector defines the level of rigor with which the contour of leaf grows (Figure 1).

Plant leaves have two different cell populations: the adaxial (or upper) and abaxial (or lower) cell populations; their boundary is considered to be important for lamina growth [7]. The morphology of leaves is highly determined by their leaf venation patterns. A classification of such patterns was carried out in [5]. We use this system and adopt its terminology. This classification system does not only consider the geometric arrangement of different vein classes but also their relation to other architectural features of leaves.

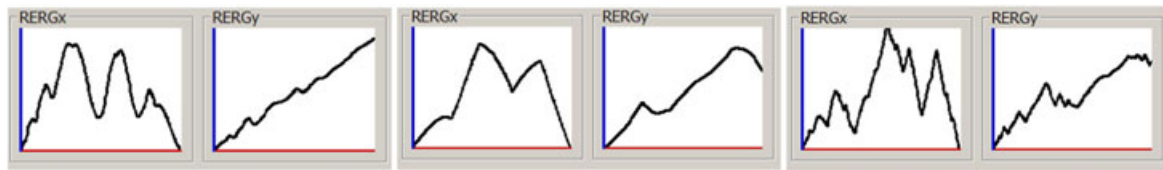


Figure 1. Axis-aligned growth curves that define three different leaves type.

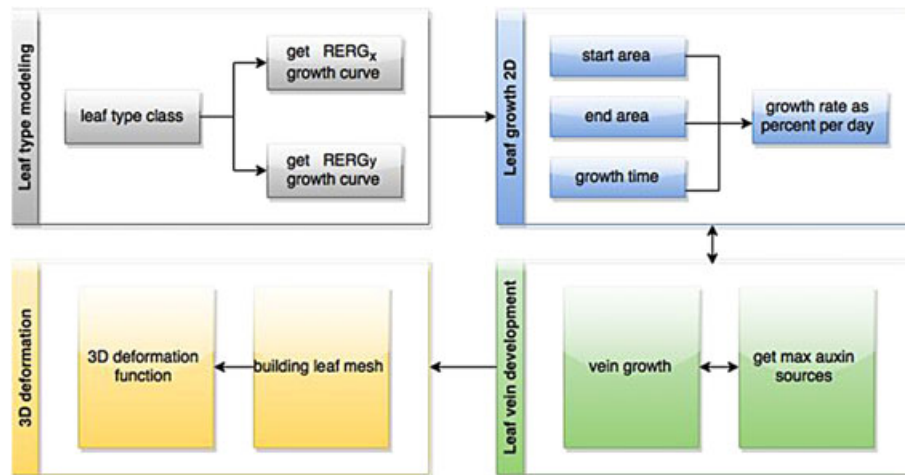


Figure 2. Leaf development is modeled by combining a 2D growth function with vein development and corresponding deformations.

Figure 2 gives an overview of our proposed method. The main aspects of our system are as follows:

- (1) A method for classifying a plant leaf by features of its contour. An image of the contour is extracted by utilizing the curvature scale space (CSS) corner detection algorithm. Every leaf is represented by the maxima of the curvature zero crossing contours of its CSS image. The similarity between two different leaves is then expressed by a real value, which is the result of comparing their CSS image representations.
- (2) Our model generates visually realistic development using the growth function  $RERG$  that lets the leaf grow towards sources of the hormone Auxin which are embedded into the leaf blade. The growth rate of plant organs is a scalar or a quantity vector depending on the desired level of precision.
- (3) A transport model based on Auxin describes a process in which initially given Auxin flows from a source to a sink while it is gradually canalized into files of cells with high levels of highly polarized transporters [8]. Our model is expressed in geometric terms and uses proximity criteria to determine the location of new primary and secondary veins. Leaf veins typically form a complex biological network [9]. Optimal networks are often trees, that is, loopless [10]; however, some leaf venation systems have a large number of closed loops (e.g., dicotyledons), which are functional and able

to transport fluid in the event of damage to any vein. Thus, in our system, higher-order veins are formed using centroidal Voronoi tessellation (CVT) and a minimum spanning tree (MST), where the size of Voronoi cells is related to Auxin quantities in these cells. The quantity of Auxin is connected to the distance between the position of the cell and secondary veins. We first generate a network of closed loops by using Centroidal Voronoi Tessellation, and then derive loopless networks (trees) by computing the Minimum Spanning Tree of the resulting Voronoi-diagram.

- (4) We represent a leaf as a triangulated double layer structure that consists of a Voronoi-diagram discretized along the veins and its corresponding diagram. The leaf mesh is mapped to deformed saddle-like mid-surface and rippled contour.

## 2. RELATED WORK

Related work for our approach encompasses biology as well as modeling methods in computer graphics.

**Biological Modeling:** The vascular system of plants consists of a network of cell files (vascular strands) that extends through all organs [8,11,12]. Over the past 20 years, genetic approaches have led to substantial increase in our understanding of leaf and vascular development, and have provided good evidence that the growth regulator Auxin provides important spatial cues for this. Because

inhibition of Auxin transport affects the formation venation patterns, Auxin is likely to be part of the involved signal [11]. In our work, we want to utilize Auxin for the visual formation of plant leaves, where the Auxin play the main role to stimulate the development and creation of venation system in our method.

Haiyi *et al.* [13] produce a model that uses geometric as well as growth control parameters to determine the shape of finite laminae. This allows for a comparative study of elongated leaf morphology. In [13], a shape space for growing elastic leaves is designed by using a combination of scaling concepts, stability analysis, and numerical simulations. This combination computes the relative growth strain. A long flat lamina deforms to a saddle shape and/or develops undulations that may lead to local ripples as the growth strain is localized to the contour of the leaf [13]. Haiyi *et al.* [14] use a combination of surgical manipulations and quantitative measurements to confirm this hypothesis and provide a simple theory for changes in the shape of a doubly curved thin elastic shell subject to differential growth across its plan-form. This functional morphology suggests new bio-mimetic designs for deployable structures with boundary or edge actuation rather than the usual bulk or surface actuation.

Hang *et al.* [15] establish phenomenological buckling models to explain the curled configuration of dried leaves. Here, the driving force is a differential contraction strain field. In this minimalistic model, the authors correlate the averaged buckling curvature to the aspect ratio and the normalized size of a leaf, as well as to the magnitude of the differential strain. Hong *et al.* [16] propose a method for modeling curly plant leaves based on venation skeletons that drive leaf surface deformation. A 2D leaf silhouette was extracted from a scanned leaf image. The algorithm computes the primary veins (medial axes) of a leaf; secondary veins were branched out automatically. SoHyeon *et al.* [17] simulate the whole leaf surface to capture the fine details of desiccated leaves. In contrast to them, we present the leaf surface as a triangulated double layer structure that consists of a Voronoi-diagram, which is constrained by the main vein structures. The leaf mesh is mapped to a deformed saddle-like leaf surface and a rippled contour.

In computer graphics, different approaches have been proposed for modeling plant leaves:

**Rule-based systems:** The first method to simulate certain patterns in nature found in plant development are L-systems [18,19]. These methods are very efficient to simulate plant organs and branching structures. Prusinkiewicz and Lindenmayer in [18] proposed many methods based on L-systems. In [20], an extension of L-systems is proposed, based on three-dimensional (3D) generalized maps that allow an easier control of the internal structure of 3D objects.

**Image-based modeling:** Quan *et al.* [21] use a semi-automatic techniques for creating plant leaves directly from images. The resulting models inherit the realistic shape and complexity of real plants. The user provides

several pictures taken from different angles; then a point cloud is built and the segmentation of individual leaves (via a graph) is done with the image information. After this, the user can manually refine the segmentation in order to bypass errors due to overlapping leaves. A generic and deformable leaf model is then applied based on this information.

**Particle systems:** Rodkaew *et al.* [22] propose a particle transportation algorithm for modeling plants in different colors and with complex venation structures. The algorithm is initiated by randomly scattered particles inside the blade of a leaf. Each particle contains energy. A transportation rule directs each particle toward a target. When particles are in close proximity, they are combined. The trails of moving particles are used to generate the venation patterns. Runions *et al.* [23] introduced a biological algorithm in order to build leaves. They use the shape of the leaf, then build veins via simulation of hormone distribution inside the leaf.

**Implicit contours:** A method designed by Hammel *et al.* [24] models compound leaves using implicit contours. This model creates a planar scalar field in the proximity of the skeleton. The margin is represented by a contour of points with a given field value. The area bounded by this contour forms the surface of the leaf. Mundermann *et al.* [25] design a method for modeling lobed leaves. This method extends the concept of sweeps to branched skeletons.

### 3. SIMULATION OF LEAF GROWTH

Photosynthesis is a process used by plants and other organisms to convert light energy into chemical energy that can be later released to fuel the organisms' activities. In order to obtain realistic leaf growth, we developed a system with four processes. The system is summarized in Figure 2.

#### 3.1. Leaf Type Modeling

The shape of the leaf blade and the type of leaf margin are important characteristics for identifying plants (Figure 3).

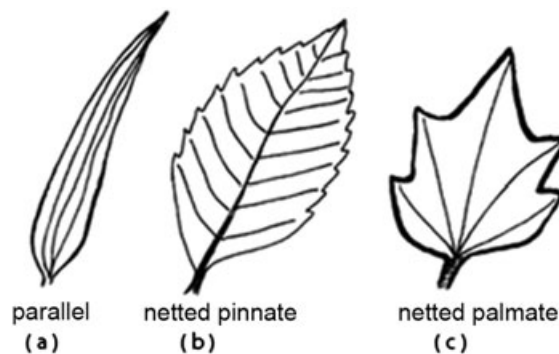


**Figure 3.** Different leaf shapes found in nature. (a) Parallel venation type. (b) Pinnate venation type. (c) Palmate venation type.

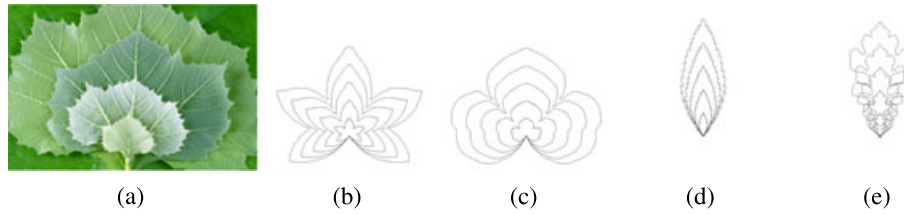


**Figure 4.** Growth of a plant leaf over time: (a) Natural growth of a plant leaf [26]. (b–e) Computer simulated growth of leaves. We started with an initial form for each type of leaf and utilized the  $\mathbb{R}ER\mathbb{G}_x$  and  $\mathbb{R}ER\mathbb{G}_y$  curve to illustrate the growth process for each leaf type.

Leaf blades vary to a large extent; they may be simple (apple and oak) or compound (divided into several smaller leaf-like segments, as in honeylocust). The smaller segments are called leaflets and are attached to a stalk (rachis) with a petiolule. Leaflets can also be arranged palmately (horse chestnut) or pinnately (ash). Pinnately compound leaves are said to be odd pinnate when ending in one leaflet (ash) and even pinnate when ending in two leaflets (locust). This terminology is important in identifying plants by their leaves.

Figure 2 shows the schematic modeling processes for leaves. Our modeling system provides the user with the ability to select an intended leaf type from various given leaf classes. After that, the modeling process starts to produce the 2D silhouette from a given input photograph, which is derived from the selected leaf type. Next, the axis-aligned elementary growth rates  $\mathbb{R}ER\mathbb{G}_x$  and  $\mathbb{R}ER\mathbb{G}_y$  are computed using the 2D silhouette. The  $\mathbb{R}ER\mathbb{G}_{l(\zeta)}$  is the rate at which an infinitesimal distance  $\Delta\zeta$  (measured in the direction of the growth line at a point on the growing silhouette) increases over time.  $\mathbb{R}ER\mathbb{G}$  is defined as [4]

$$\mathbb{R}ER\mathbb{G}_{l(\zeta)} = \left( \frac{1}{\Delta\zeta} \right) \left( \frac{d\Delta\zeta}{dt} \right). \quad (1)$$

Using the  $\mathbb{R}ER\mathbb{G}$ , we create a growth curve (vector valued) for the  $\mathbb{X}$  and  $\mathbb{Y}$  coordinates of each leaf type (Figure 1).

In order to produce different growth curves for same leaf type, we use a merging algorithm between growth curves that belong to the same leaf type. From this algorithm, we may get different leaf forms for the same plant, for example, when having two growth rate vectors  $\mathbb{R}ER\mathbb{G}_{x1}$  and  $\mathbb{R}ER\mathbb{G}_{x2}$  for a single leaf type, the new growth rate  $\mathbb{R}ER\mathbb{G}_{xm}$  is computed by combining both vectors.

### 3.2. Leaf Expansion

To simulate leaf growth, we use a 2D model because the thickness of a leaf can be considered negligible compared with the growth of its surface. Under these assumptions, the surface expansion is modeled by an expansion rate (percent per day)  $GR$  [3]:

$$GR = 100 * \left[ e^{(\ln(S_{area}/E_{area})/t)} - 1 \right], \quad (2)$$

where  $S_{area}$  and  $E_{area}$  are leaf area at two different measurements and  $t$  equals the number of days between measurements. The growth model used in this paper has been tested on several types of leaves. We observed that various parts of the leaf lamina expand at different rates, depending on their distance to the tip and the age of the leaf. Figure 4(a) illustrates the growth of a natural leaf while in 4(b)–(e) computer simulations are shown using the expansion rate  $GR$ . Our results resemble natural growth quite faithfully.

### 3.3. Determination of Auxin Sources and Maxima

Our algorithm distributes Auxin sources at leaf edges and simulates the venation process based on the Auxin level and consumption. Strong Auxin sources are assumed to exist at edge locations that grow faster than others [27]. Figure 5 illustrates the relationship between the venation patterns and maximum Auxin sources.

We used the Shi-Tomasi corner detector and features [28] to track the max Auxin placement at the leaf contour, which we get from the input photography. The growth in

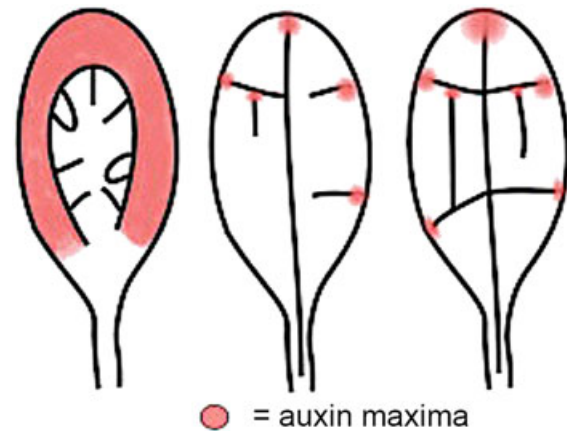


**Figure 5.** Illustration of the relationship between Auxin maxima (red points) and primary and secondary venation processes (black curves). The left image illustrate how and where the Auxin are distributed through the blade of leaf. Both another images show the development of primary and secondary venation processes related to maxima Auxin.

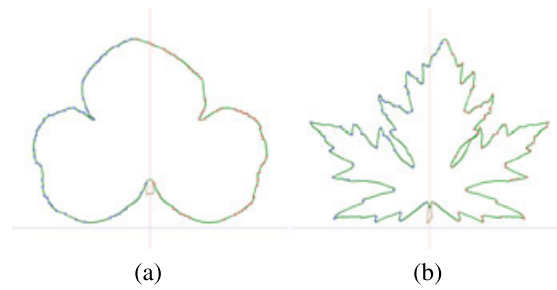


**Figure 6.** Maxima for the Auxin distribution for two leaf types. The red and blue points are to explain the positions of max Auxin at the leaf edge.

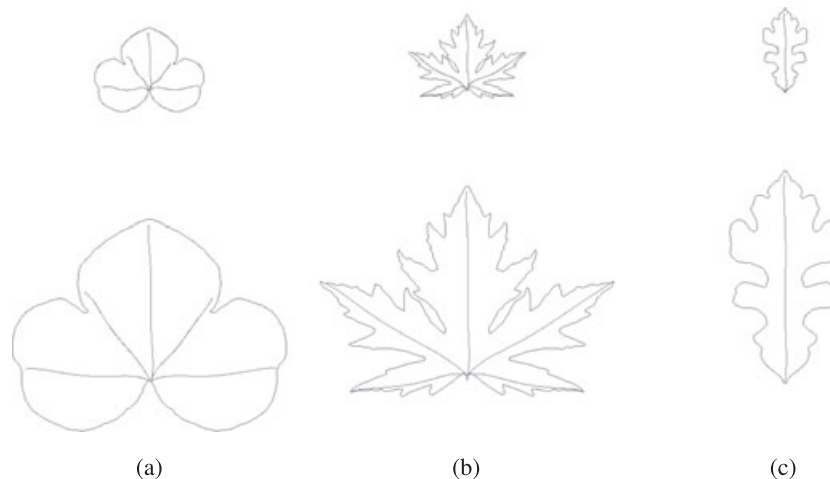


**Figure 7.** Development of primary veins with respect to localization of max Auxin. The first row illustrates the canalization process for primary veins; the second row illustrates the development of primary veins after some time.

each leaf corner must be larger than for other leaf locations. Therefore, we deduce Auxin maxima to be located at leaf corners. In Figure 6, the red and blue circle represent such sources.

### 3.4. Generating and Growing the Venation System

The plant growth regulator Auxin is also to be responsible for the development of the venation patterns [11]. For most leaves, the primary and secondary veins are not only the most obvious features but also play the most significant role in leaf deformation. Therefore, we concentrate on simulating growth and development of primary and secondary veins. Our algorithm, however, can also simulate third and subsequent levels of veins.

During initial leaf growth, a small primordium becomes visible at the flanks of the shoot apical meristem. Epidermal Auxin flow converges to form a maximum of Auxin activity at the tip of the primordium. It is drained through the center of the primordium, marking the position of mid vein of the new leaf. In primary morphogenesis, leaves grow predominantly via cell division to acquire their shape and vascular pattern. Auxin maxima at the margins of

the leaf correlate with sites of lateral vein formation and positions of serration development.

We generate the primary veins related to the given leaf type and the maximum of Auxin sources. Maximum of Auxin are assumed at locations that have a growth rate above a given threshold. Next, channels between maximum Auxin sources and the center positions are built. Figure 7 illustrates the development of primary veins with respect to maximum Auxin concentrations at the leaf margin.

In order to generate the secondary veins, we firstly develop a function to choose a parametric number  $n$  of nodes in each primary vein. Then, we search for  $n$  Auxin sources in the leaf margin. Each Auxin source is now assumed to join the vein node closest to it. In Figure 8, we simulate the development process of primary and secondary veins with respect to Auxin maxima at the leaf boundary. As shown in Figure 9, the natural venation systems in column (a) and our computer simulated venation systems in column (b) are quite similar.

### 3.5. Higher-order Venation Patterns

For our needs, we developed an interface to automatically generate complex venation systems from a leaf skeleton

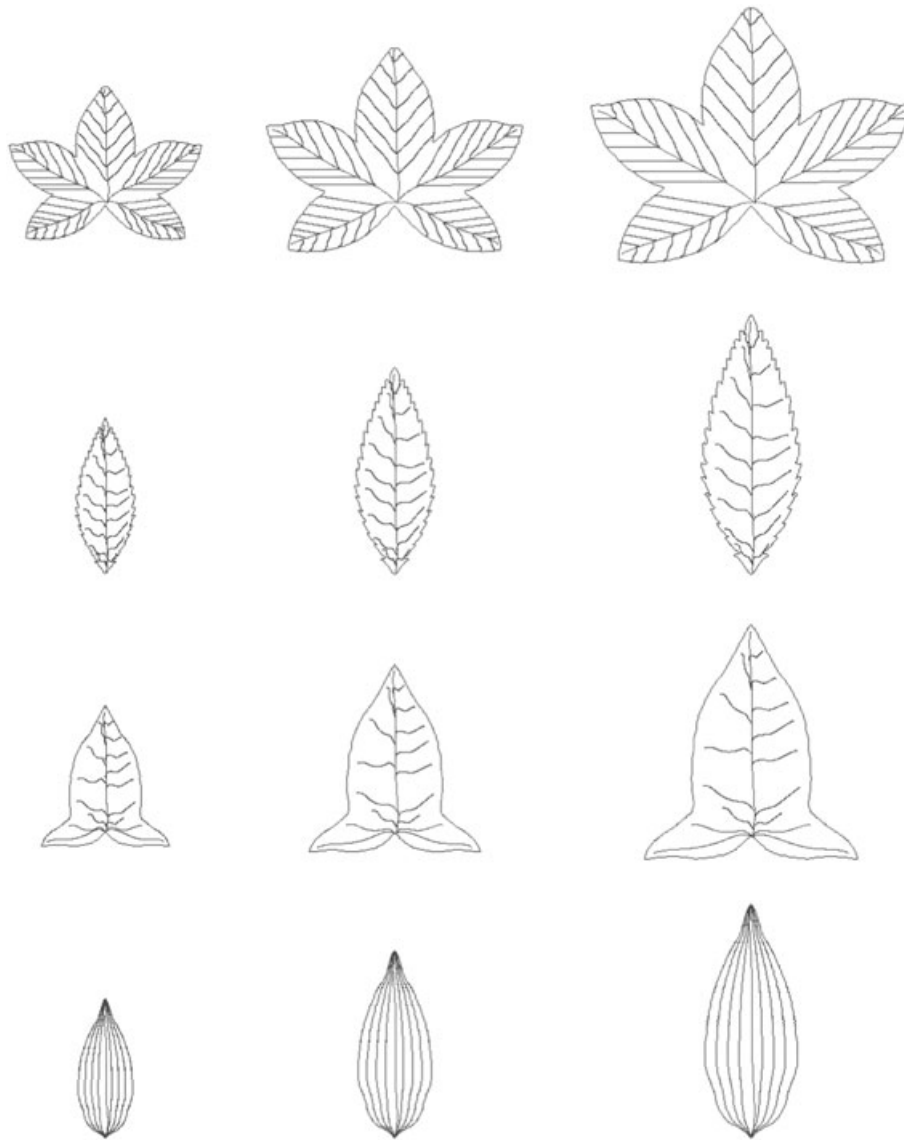


**Figure 8.** Development of primary and secondary veins with respect to localization of max Auxin for several leaf type.

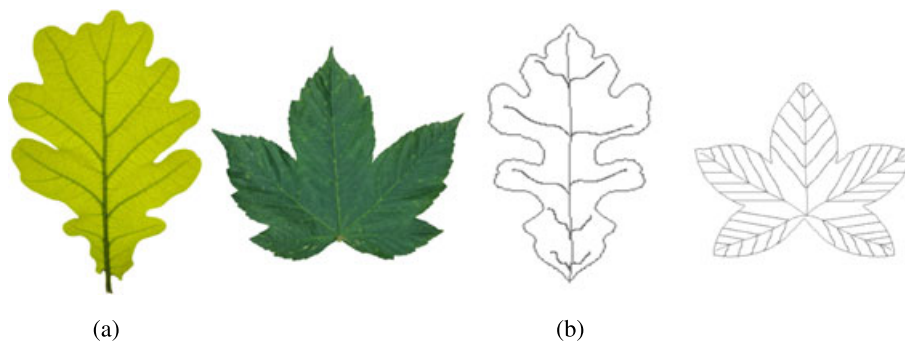


**Figure 9.** Comparison of natural venation systems [26] and our venation systems. Our system can use many of Bezier curves to draw the first and second veins.

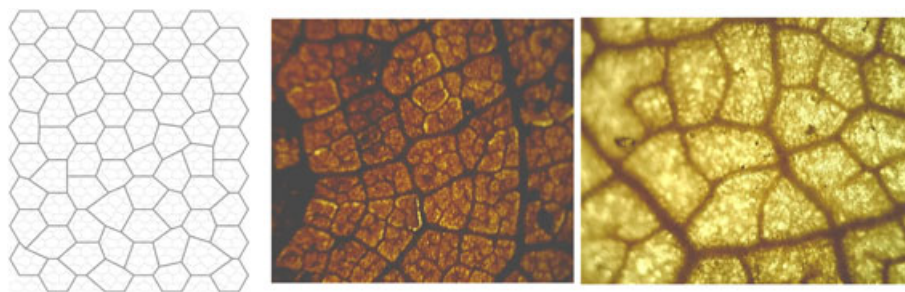


**Figure 10.** Illustration of the third level of natural venation system [26]. (a) Voronoi-diagram, (b) minimum spanning tree of Voronoi-diagram, (c) minimum spanning tree and Voronoi-diagram.

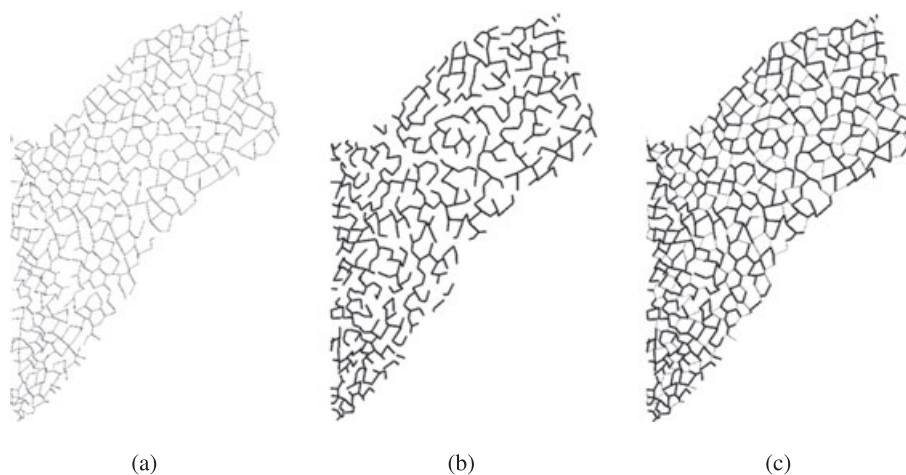


**Figure 11.** Illustration the third and higher level of our produced venation system.

by using Voronoi-diagrams. As shown in Figure 10, large cells are distributed along the leaf surface that consists of smaller ones; with sufficient magnification, it is visible that even the cells between veins are deployed as Voronoi tessellations.

In order to create third and higher-order veins (Figure 11), we start with a set of randomly distributed points of Auxin sources that are distributed in a blue noise distribution [29]. All points must lie within the region formed by two second-order veins. Additionally every point has a weight, which is related to the quantity of Auxin at this location.

The so-called CVT [30] simulates the segmentation of cells on the leaf; see Figure 11(a). The CVT is considered as a connected weighted graph. In the next step, we utilize an algorithm (JGraphT is a free Java class library that provides mathematical graph-theory objects and algorithms) to get minimum spanning tree of this graph; see Figure 11(b). We find a subset of edges that form a tree that includes every vertex, where the total weight of all the edges in the tree is minimized. The presented tree provides a useful simulation of the venation patterns. Finally,

we join together all the edges, which are produced from CVT with the edges, which are produced from the MST in order to present the final form of veins (Figure 11(c)).

### 3.6. Building the Leaf Mesh

In the previous steps, we have constructed a leaf skeleton using two boundary curves and a central vein curve. To mesh the not yet existing area within these boundary curves, we employ Delaunay triangulation to get the leaf mesh. Using produced mesh, we can deal with concave areas in the leaf; see Figure 12. For example, lobed leaves often have irregular silhouettes characterized by a number of concave outlines.

Generally, each vein-point is inserted as a new vertex into the leaf mesh in order to link mesh triangles with the veins. The leaf mesh is textured with different colors such that each color is related to the position and the type of the vertex, where a texture is utilized as a color plate to get different colors. In addition, the leaf contour is prepared separately, and then it is linked to leaf mesh.

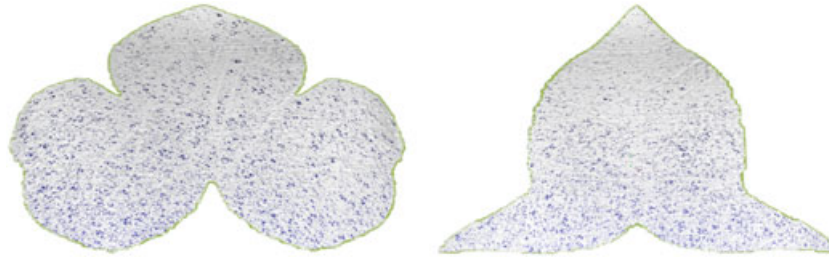


Figure 12. Two leaf meshes.

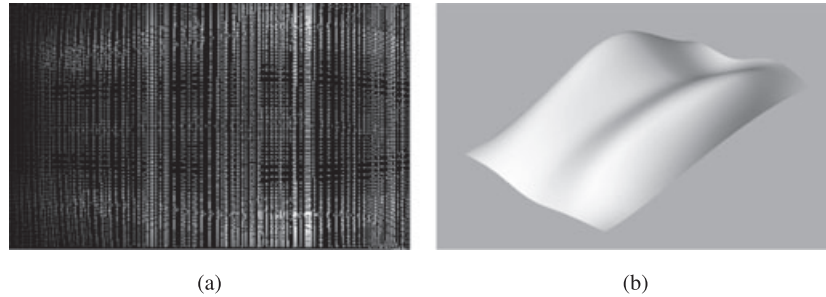


Figure 13. Characterization of 2D and 3D deformation shape function.



Figure 14. Characterization our venation system with leaves grow. Here, we use  $N_i$  cells for each area between two neighbored second veins.

### 3.7. 3D Deformation Function

Leaves and flowers usually have a typical, saddle-like mid-surface and a characteristic rippling pattern at their edges. To produce a saddle shape, we propose the function

$$\tau(x, y) = \lambda(x + y)^2 - \mu(x - y)^2, \quad (3)$$

where  $0 \leq \lambda \leq 1$  and  $0 \leq \mu \leq 1$  are constants. This function fulfills all the arithmetic conditions [13] and has the shape of a saddle, as shown in Figure 13(b). To represent ripples and its physiological role during leaves growth, we use a function  $\varphi$  for periodic rippling [13]:

$$\varphi(x, y) = \delta(y)\sin(kx), \quad (4)$$

Here  $k$  is a dimensionless wave number, and  $\delta(y)$  is the cross-sectional profile of the surface.

In Figure 13, we show the resulting 2D and 3D deformation shapes from saddle and rippling functions. In order to get a 3D deformed leaf surface, we utilize the deformation function illustrated in Figure 13. Our system can create several deformation shapes from different deformation functions. In addition to that, each leaf type has its own deformation function.

## 4. MODELING RESULTS

We implemented our system using C++, OpenCV, OpenGL, and the QT library. Firstly, we produced the growth curve for several leaf types. Figure 1 shows different plots of growth curves that have been used to simulate the growing of leaves. Equation (1) represents a growth curve using  $x$  and  $y$  coordinates for each leaf type. The surface expansion is modeled by an expansion rate in the form

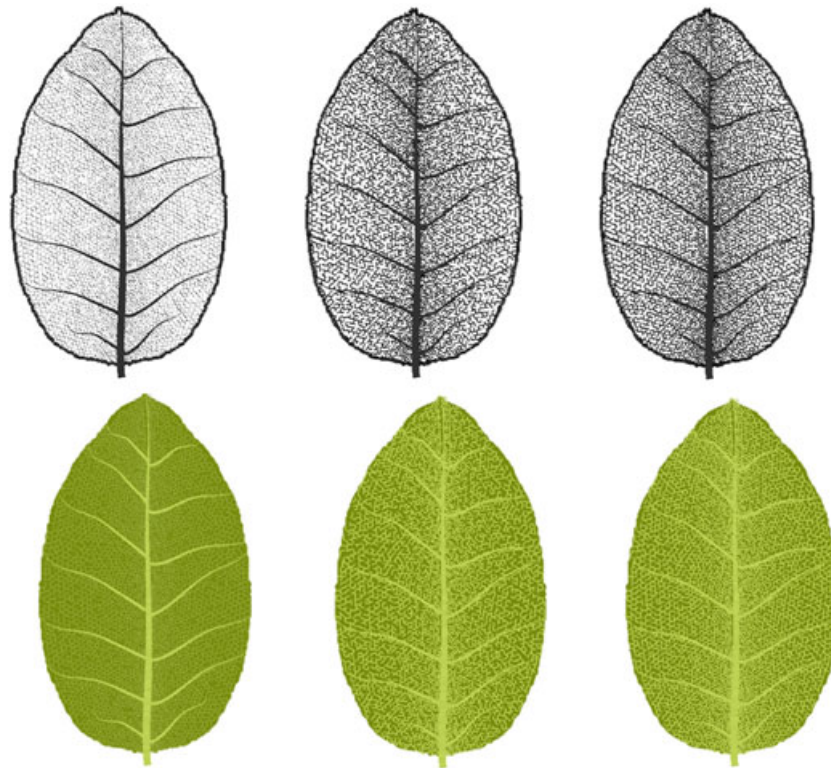


**Figure 15.** Illustration of the third and higher level of our venation system for all leaf sections.

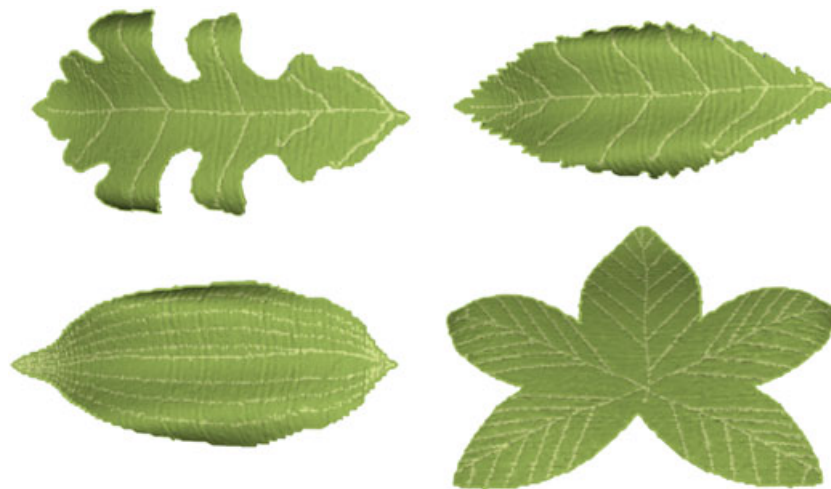


**Figure 16.** Our system allows for the simulation of various types of leaves including different venation patterns and complex leaf shapes.

of percent per day  $GR$ ; see Equation (2). The growth of a plant leaf during a time period is simulated in Figure 4, which shows in (a) the natural growth of a plant leaf, and in (b–e) computer simulated growth of a plant leaf.

Our algorithm detects the placement of maximum Auxin sources at leaf edges using Shi-Tomasi corner detector. Figure 6 illustrates the algorithm to determine the maximum Auxin distribution for several types of leaves.

After identifying the leaf type, maximal Auxin placement, and number of primary veins, we generate the primary venation development system for several leaf types. Figure 7 illustrates the development of primary veins with respect to the locations of Auxin maxima at the leaf boundary. The development of primary and secondary veins is simulated in Figures 9 and 8.

We generate realistic leaf venation systems for third and higher level veins by using CVT and MST; see Figure 15. Our algorithm distribute the  $N_i$  ( $N_i$  is number of cells in the area between two neighbored second veins, see Figure 14) points using Blue Noise point distributions for each section between second-order veins. Here,  $N_i$  related to the leaf mass per area [31]. Additionally, each created point has a weight related to the Auxin level at the position of the point. When the point is more far from the secondary veins, the quantity of Auxin (weight of point) is larger. Figure 14 illustrates the development of the third-order venation system for a growing leaf. At each step of development, some new cells are added (Figure 15). An MST on the resulting Voronoi graph is used to profuse the structure of third-order veins; see Figure 15.

The leaf surface is generated within boundary curves using Delaunay Triangulation. Our system creates several deformation shapes generated from many different created deformation functions used to deform the leaf shapes; see Figure 13. Then, we texture the leaf with different colors; see Figure 16. Compared with previous related work on modeling and simulating growth of leaves, our method is motivated by all growth stages from biology and ecology science in order to get a natural modeling of several leaf development types.

## 5. FUTURE WORK

We presented an automatic technique for constructing realistic leaf models for several leaf types. We showed how to model 2D natural growth for several types of leaves and illustrated 3D renderings of deformed results. In the future, we plan to integrate the simulation of different outer and inner effects on the leaves, such as cracks, insect attacks, and growing spots. Additionally, we are going to draw the growth system of leaf edge and of venation system more asymmetric growth in order to get more realistic system. Finally, there are many more natural phenomena that happen with leaves, which we plan to simulate.

## ACKNOWLEDGEMENTS

The work reported here was supported in part by the Institute of International Education and its Scholar Rescue Fund, by National Foreign 1000 Talent Plan (WQ201344000169) and Leading Talents of Guangdong Program (00201509), and by NSFC with Nos. 61501464 and 61331018.

## REFERENCES

1. Prusinkiewicz P. Visual models of morphogenesis. *Artificial Life* 1994; **1**(1–2): 61–75.
2. Wang IR, Wan JWL, Baranoski GVG. Physically based simulation of plant leaf growth. *Computer Animation and Virtual Worlds* 2004; **15**(3–4): 237–244.

3. Coley PD, Bateman ML, Kursar TA. The effects of plant quality on caterpillar growth and defense against natural enemies. *Oikos* 2006; **115**(1–2): 219–228.
4. Hejnowicz Z, Romberger JA. Growth tensor of plant organs. *Journal of Theoretical Biology* 1984; **110**(1): 93–114.
5. Nebelsick AR, Uhl D, Mosbrugger V, Kerp H. Evolution and function of leaf venation architecture. *Oxford Journals* 2001; **87**(5): 553–566.
6. Coen E, Rolland-Lagan AG, Matthews M, Bangham JA, Prusinkiewicz P. The genetics of geometry. *Proceedings of the National Academy of Sciences* 2004; **101**(14): 4728–4735.
7. Nakata M, Okada K. The leaf adaxial-abaxial boundary and lamina growth. *Plants* 2013; **2**(2): 174.
8. Rolland-Lagan AG, Prusinkiewicz P. Reviewing models of auxin canalization in the context of leaf vein pattern formation in arabidopsis. *The Plant Journal* 2005; **44**(5): 854–865.
9. Corson F. Fluctuations and redundancy in optimal transport networks. *Physical Review Letters, American Physical Society* 2010; **104**(4): 048703.
10. Katifori E, Szllsi GJ, Magnasco MO, Gergely J, Marcelo O. Damage and fluctuations induce loops in optimal transport networks. *Physical Review Letters* 2010; **104**(4): 048704.
11. Scarpella E, Barkoulas M, Tsiantis M. Control of leaf and vein development by auxin. *Cold Spring Harbor Laboratory Press* 2010; **2**(14): 4728–4735.
12. Bilsborough GD, Runions A, Barkoulas M, Jenkins HW, Hasson A, Galinha C, Laufs P, Hay A, Prusinkiewicz P, Tsiantis M. Model for the regulation of arabidopsis thaliana leaf margin development. *PNAS* 2011; **108**(8): 3424–3429.
13. Liang H, Mahadevan L. The shape of a long leaf. *PNAS* 2009; **106**(52): 22049–22054.
14. Liang H, Mahadevan L. Growth, geometry, and mechanics of a blooming lily. *PNAS* 2011; **108**(14): 5516–5521.
15. Xiao H, Chen X. Modeling and simulation of curled dry leaves. *Soft Matter* 2011; **7**(48): 10794–10802.
16. Xu H, He D. Venation-skeleton based curly leaf modeling. *Advances in Information Sciences and Service Sciences* 2012; **4**(6): 52–60.
17. Jeong SH, Park S-H, Kim C-H. Simulation of morphology changes in drying leaves. *Computer Graphics Forum* 2013; **32**(1): 204–215.
18. Prusinkiewicz P, Lindenmayer A. *The Algorithmic Beauty of Plants*. Springer-Verlag New York, Inc.: New York, NY, USA, 1996.

19. Rodkaew Y, Lursinsap C, Fujimoto T, Siripant S. Modeling leaf shapes using l-systems and genetic algorithms. In *International Conference NICOGRAPH (April)*, 2002; 73–78.
20. Terraz O, Guimberteau G, Mérillou S, Plemenos D, Ghazanfarpour D. 3gmap l-systems: an application to the modelling of wood. *Visual Computer* 2009; **25**(2): 165–180.
21. Quan L, Tan P, Zeng G, Yuan L, Wang J, Kang SB. Image-based plant modeling. In *ACM SIGGRAPH 2006 Papers, SIGGRAPH '06*. ACM, New York, NY, USA, 2006; 599–604.
22. Rodkaew Y, Chongstitvatana P, Siripant S. Modeling plant leaves in marble-patterned colours with particle transportation system, 2004.
23. Runions A, Fuhrer M, Lane B, Federl P, Rolland-Lagan A-G, Prusinkiewicz P. Modeling and visualization of leaf venation patterns. *ACM Transactions on Graphics* 2005; **24**(3): 702–711.
24. Hammel M, Prusinkiewicz P, Wyvill B. Visual computing: integrating computer graphics with computer vision. In *Proceedings of Computer Graphics International 92*, Kunii TL (ed.). Springer-Verlag: Tokyo, Japan; 119–212, 1992.
25. Mundermann L, MacMurchy P, Pivovarov J, Prusinkiewicz P. Modeling lobed leaves. In *Proceedings of Computer Graphics International, 2003*. IEEE, Tokyo, Japan, 2003; 60–65.
26. Digital pictures of all sorts of materials. Available online at [www.textures.com/](http://www.textures.com/).
27. Stanko V, Giuliani C, Retzer K, Djamei A, Wahl V, Wurzinger B, Wilson C, Heberle-Bors E, Teige M, Kragler F. Timing is everything: highly specific and transient expression of a {MAP} kinase determines auxin-induced leaf venation patterns in arabidopsis. *Molecular Plant* 2014; **7**(11): 1637–1652.
28. Shi J, Tomasi C. Good features to track. In *1994 IEEE Conference on Computer Vision and Pattern Recognition (CVPR'94)*, Seattle, WA, 1994; 593–600.
29. Ulichney RA. Dithering with blue noise. *Proceedings of the IEEE* 1988; **76**(1): 56–79.
30. Rong G, Jin M, Guo X. Hyperbolic centroidal voronoi tessellation. In *Proceedings of Symposium of Solid and Physical Modeling (SPM 2010)*. Digital Equipment Corp., Hudson, MA, USA, 2010; 117–126.
31. Castro-Diez P, Puyravaud JP, Cornelissen JHC. Leaf structure and anatomy as related to leaf mass per area variation in seedlings of a wide range of woody plant species and types. *Oecologia* 2000; **124**(4): 476–486.

## AUTHORS' BIOGRAPHIES



**Monssef Alsweis** received his PhD degree in computer graphic application from the Department of Computer and Information Science, Konstanz University, in 2007. Now he is visiting research scholar at Konstanz University. He teaches at Konstanz University the following courses: Virtual and Augmented Reality and Aktuelle Trends in der Computergrafik. His research interests are modelling and visualisation of plants and visualisation of complex data structure.



**Oliver Deussen** graduated at Karlsruhe Institute of Technology (Germany) in 1996 and was postdoctoral researcher at University of Magdeburg. In 2000, he was appointed a professor for Computer Graphics and Media Design by Dresden University of Technology. Since 2003, he is professor for Computer Graphics and Media Informatics at Konstanz University. He was guest researcher at Microsoft Research (USA) and is Visiting Professor at the Chinese Academy of Science (SIAT Shenzhen). In 2014, he was awarded within the 1000 talents plan of the Chinese Central Government. As vice president of Eurographics Association and co-editor in chief of Computer Graphics Forum, he helps fostering computer graphics research in Europe. His areas of interest are modelling and rendering of complex objects, non-photorealistic rendering as well as information visualization.



**Jia Liu** received her PhD degree in computer application from the Institute of Automation, Chinese Academy of Science (CAS) in 2010. Now she works at School of Automation, Beijing Information Science and Technology University. Her research interests include pattern recognition and 3D modelling.